"Physics of Auroral Phenomena", Proc. XXXI Annual Seminar, Apatity, pp. 37 - 41, 2008

Polar Geophysical Institute

THE 14 SEPTEMBER 2004 SUBSTORM: ESTIMATING PARAMETERS OF THE CROSS-TAIL CURRENT DISRUPTION REGION

V. Mishin, M. Tolochko, L. Sapronova, Yu. Kuzminykh, M. Kurikalova *(Institute of Solar-Terrestrial Physics SB RAS, Irkutsk, Russia)*

Abstract. [1]. We admit that a couple of field-aligned currents (FAC) of the classic substorm current wedge (SCW) is closed by the dusk-to-dawn current in the plasma sheet of the near- and midtail, and that the mentioned current disrupts the tail main current flowing dawn-to-dusk. We set a simple model of the disruption region, and admitted that the intensity of the disturbing current, J, is equal to the intensity of FAC, inflowing in the dawn sector of the ionospheric projection of SCW. On such a basis, using the 14 Sep 2004 substorm data, we calculated the values of J, also components J_x and J_y along and across the tail, respectively. For this purpose, by means of the magnetogram inversion technique, maps of the FAC density spatial distribution in the polar ionosphere were calculated. We made calculations separately for the two subsequent phases of the substorm - the pseudobreakup phase (PSR), and the following expansion phase (TLR). We noted that the PSR development in the near tail and sudden expansion of disturbance to the mid- and distant tail both were stimulated by the IMF turning northward. In the SCW current disruption region of the trail, the condition for the dynamo-region, $\mathbf{j}\cdot\mathbf{E} < 0$, is satisfied. Further, we obtained estimates of the disrupted magnetic field (B), induction emf (ΔU), and disturbance power (Q_{scw}). As disturbances in the PSR region do not cease, but even increase during the TLR, we also obtained the J and Q_{scw} values, and the values of B, ΔU separately for the PSR and TLR areas, and on the PSR+TLR aggregate area. We found that all the four - J, B, ΔU and Q_{scw}- values for the time interval and on the PSR+TLR area manyfold or by an order of magnitude more than for the time interval and in the PSR area.

1. Introduction

[2] There are several main semiempirical models of a substorm, which are actively discussed in the literature as alternative and/or complementary to one another. The discussion focus in recent ~ 20 years and nowadays is the issue of one or two active phases of a typical substorm. In the NENL model the main active phase is formed by large-scale reconnection of the open lobe magnetic flux in the mid- and distant tail [Baker et al., 1996; 2002]. In the CD model, the main active phase is a small-scale reconnection of the closed magnetic field in the near tail plasma sheet [Lui, 2002; 2003; 2007]. In the model [e.g., Lyons et al., 1997; Lee, Lyons et. al., 2007], the main substorm active phase is created by the IMF turning northward. Modification and synthesis of the listed approaches, based on the observational data, are actively discussed but remains an actual task [e.g., Mishin et al., 2001; Nakamura et al., 2006; Cheng et al., Caumans et al., 2007; Cao, Pu, et al., 2008; and references therein]. The goal of this paper is to obtain new data, supporting the mentioned synthesis. In a substorm we detect the pseudobreakup phase and the following expansion phase, designating these two phases as PSR (Plasma Sheet Reconnection - the CD analog) and TLR (Tail Lobe Reconnection - the TLR analog) [Cao, Pu, et al., 2008]. Admitting that both phases are formed by the partial or complete disruption of the tail current, we obtained in this paper, separately for the PSR and TLR periods, estimations of some parameters of disruption regions, including the values of the disrupted magnetic field and disruption process power. In fact, the second active phase of the non-isolated substorm considered is the PSR+TLR phase since disturbances in the PSR region do not cease, but increase during TLR.

[3] The paper is based on the assumption that the couple of field-aligned currents (FAC) of classic substorm current wedge (SCW) closes the dusk-dawn current, which is opposite to the main cross-tail current in the plasma sheet, and that the closing current creates the main current disruption mentioned above. We suppose that the closing current with the intensity J can have the dusk-dawn components Jy and the component Jx along the tail, and that the intensity J is equal to the intensity of the FAC flowing downward into the polar ionosphere in the dawn sector of the ionospheric projection of the SCW. We calculated the 2D-maps of the FAC density spatial distribution in the polar ionosphere, determined the J values, the position of D and U centers for the downward and upward (from the ionosphere) SCW FAC, and the J_y and J_x values. Further we introduced a number of simplifying assumptions which, together with the FAC data, provided calculation of the tail current disruption region parameters.

2. Database and Timing

[4] We use 2D-maps of the FAC density spatial distribution in the ionosphere, the equivalent ionospheric currents and electric potential maps, all of them calculated in increments of 1-5 minutes on the basis of the magnetogram inversion technique, MIT [Mishin et al., 1986; 1990; and references therein]. The MIT input data were obtained from 117 ground-based magnetometers at $\Phi > 40°$. By using these data, we determined the polar cap boundaries, the open magnetic flow (Ψ) through it, the Harang discontinuation center MLT (t_w). On the maps of the SCW FACs we determined the centers of the downward (D) and outward (U) FACs. Also, we used the AE indices, calculated by data of 55 magnetometers at $\Phi > 60°$, and solar wind parameters at ACY [CDAWeb, Goddard Space Flight] (Figure 1). Calculations were carried by using data of the 14 Sep 2004, (17-21) UT substorm interval. A part of this interval was investigated earlier after Cluster data by Cao, Pu, et al [2008]. The mentioned interval was selected from Cluster data. This

interval contains the non-isolated substorm in the storm's middle.

[5] The ACY data are shown in Figure 1 with the delay $\tau=X_{ACY}/V_{sw}$. Vertical lines mark substorm onsets during the predicted PSR (one asterisk, pseudobreakups) and TLR (two asterisks, expansion onsets) phases. For timing we used the ACY data, Ψ and t_w plots, the data from X-records of the groundbased magnetometers, which, at 18-19 UT, were in the near-midnight sector of the auroral oval, as well as the plots of the SCW FAC intensity and latitude of D and U SCW FACs centers. According to [Nakamura et al.,1994; Koskinen et al. 1993], the pseudobeakups are comparatively weak magnetic bays in the low-latitude portion of the oval, observed (in the isolated substorms) at the Ψ growth substorm's phase [Mishin et al. 1997; Rostoker, 1998]. In the non-isolated substorm under consideration, the latter is not entirely so (Figure 1). The plot of Ψ is not reliable because of strongest twisting of the observed spatial distribution of the FACs density in the ionosphere (see Figure 4). The expansion onsets/TLR phase is marked as the pseudobeakups/PSR phase prolongation. Its onset coincides with the spontaneous increasing amplitude of the magnetic bays in the near midnight auroral oval [Mishin et al., 2008] and accompanied by spontaneous strong increasing of the SCW FAC intensity (Figure 3) and by expansion of the disturbance region towards high latitudes (Figure 2).

[6] In this paper, due to its limited space, we show only a portion of the mentioned data. In Figure 1, the ACY data, Ψ, t_w, and AE-indices plots are shown. In Figure 2 we give the plot of the SCW FACs two centers' mean latitude change during the substorm. This plot illustrates the drift to the pole of the SCW FACs common center, observed at the transition from PSR to TLR.In Figure 3 we show the plot of the SCW intensity (J) spontaneous change, admitting J to be equal to the intensity of the SCW downward FAC, J_+. In Figure 4 we present the maps of the FAC density spatial distribution, obtained by averaging the PSR and TLR phases. We show the position of the D and U centers, we mark the α angle between the tangent to the geomagnetic parallel in the D point and the direction from D to U. By measuring this angle and the distance between D and U, and by averaging J values in Figure 3 separately for PSR and TLT phases, we obtained approximate $J_y=J\cdot\sin\alpha$ and $J_x=J\cdot\cos\alpha$ values, where the X and Y axes are sunward and dawn-dusk, respectively. The reader will find some additional data and description of the processing techniques in the paper Mishin et al. [2008].

[7] The data from Figures 1-3 are interpreted in this paper as evidence of the PSR regime before 1825 UT and sudden transition to the TLR regime near 1825 UT, soon after the northward turn of IMF.

3. Model

[8] We admitted simplifying assumption that the J_+ intensity of the SCW downward FAC is equal to the intensity J of the current flowing to the ionosphere from the disruption region of the main current of the plasma sheet tail (assumption A), and that the tail current has the above-mentioned J_y and J_x components (assumption B). We also admitted that the tail current, and the oppositely directed disrupting SCW dusk-down current in the disruption region, both flow in a thin sheath near the tail neutral sheath, and the current sheath is only ~ 0.1 R_E thickness [e.g., Nakamura et al., 2006].

We used the two-dimensional model of this disrupting Thin Current Sheath (TCS) in which $\partial/\partial z=0$ (assumption D) is met, and the equations are true

$$\text{rot } B = \mu_0 j \quad (1)$$

$$\Delta F/\Delta t = -\Delta U \quad (2)$$

$$Q = J\cdot\Delta U \quad (3)$$

where $\mu_0=4\pi\cdot10^{-7}$ Weber / (Ampere·meter)**, j, B,** F, ΔU, and Q, are, respectively, the disrupting current density, disrupted magnetic field, magnetic flux through the disruption region, Emf in the contour framing the disruption region, and power dissipated in the SCW (all parameters are given in SI units). Admitting the condition $\partial/\partial z=0$ in the TCS, from (1) we obtain B=Bz, Bx=0.

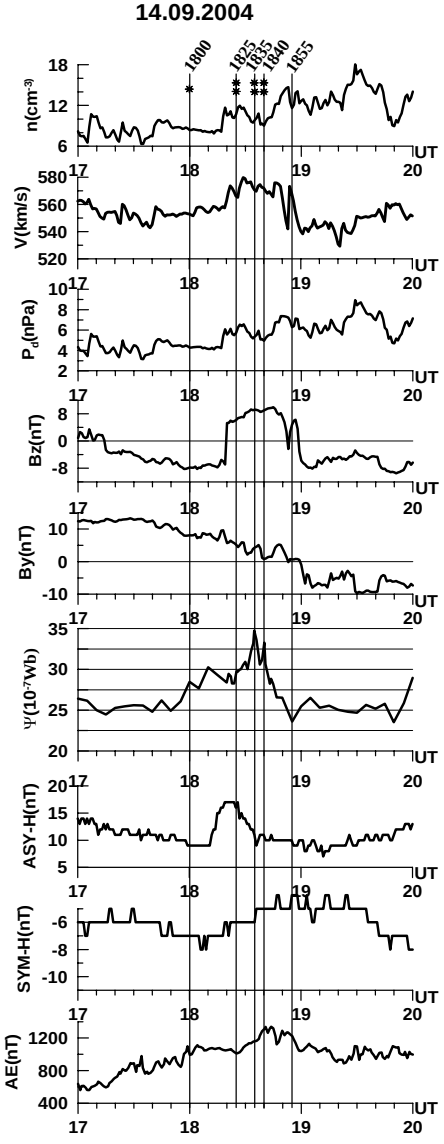

Figure 1. The ACY data, Ψ, t_w, and AE-indices plots are shown.

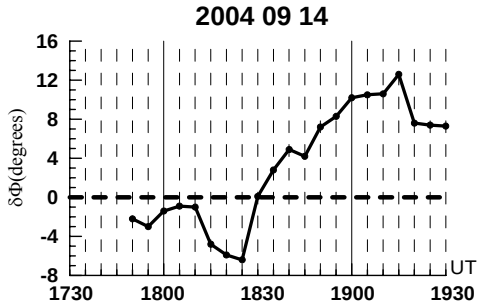

Figure 2. $\delta\Phi$ is the mean latitude of D- and U-centers of the downward and upward SCW FACs (see Figure. 4).

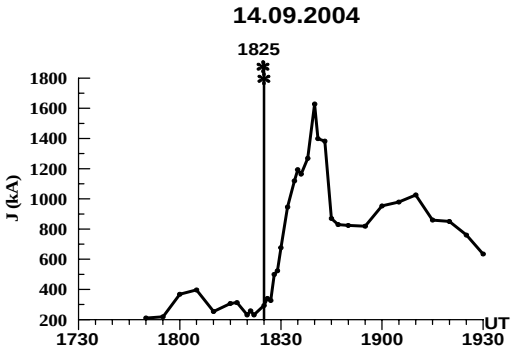

Figure. 3. The plot of the SCW intensity (J) variation. (The value of J is admitted to be equal to the intensity of the SCW downward FAC, J_+).

Figure 4 The maps of the FACs density spatial distribution in the coordinates geomagnetic latitude and MLT. Downward (upward) FAC – the dashed (solid) isocontours. The boundaries of the Iijima-Potemra's (I-P) FAC Regions are shown, and the two meridians, limiting the SCW FACs of I-P Region 1. See text for more details.

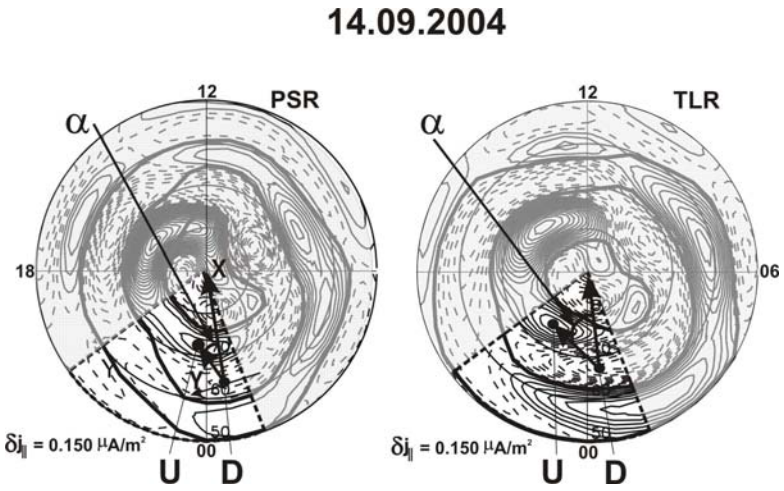

Also admitting that the disruption region is a rectangle with the X and Y size (assumption E), from the equations (1) - (3) we obtain the equations for J_y:

$dBz/dx=-\mu_0 j_y$ (4)

$j_y=(J\cdot\sin\alpha)/(XY)$ (5)

$|Bz_y|=(\mu_0 J\cdot\sin\alpha)/Y$ (6)

$\Delta F_y=\mu_0\cdot J\cdot\sin\cdot\alpha\cdot X$ (7)

$Q_y= (\mu_0\cdot J^2\cdot\sin\cdot\alpha\cdot X)/\Delta t$ (8)

$\Delta U_y= (\mu_0\cdot J\cdot\sin\cdot\alpha\cdot X)/\Delta t$ (9)

Here the x and y subscripts designate the Bz, j, F, Q, and ΔU parameters, referring to the J_x and J_y currents, respectively, Δt is the disturbance development time, calculated by the groundbased X-magnetograms and plots Figure 1: $t_1=6\cdot10^2$ sec for PSR, $\Delta t_2=1.2\cdot10^3$ sec for TLR.

[9] In the model applied, the disruption region of the SCW is a rectangle in the equatorial plane with the area, $S_1= X_1.Y_1$, where$Y_1=X_1=10$ R_E and $-5 \geq x \geq -15$ R_E for PSR. X_1 and Y_1 are supposed to be constant values, since $\Delta\Phi\approx$const in the interval of the initial PSR (Figure 2). For the PSR+TLR spatial area we admit that the general area is $S_2=S_1+\Delta S$, where $\Delta S =\Delta X\cdot\Delta Y$, $\Delta X=20$ R_E and $-15\geq x \geq -35$ R_E. These rough estimates are partially based on mapping the FAC spatial distribution into the equatorial plane, using the T-96 model. They are in agreement with the estimates by Lu et al. [2000], and do not contradict to other data from the literature [e. g., Miyashita et al., 2004; Nagai et al., 1998; Birn and Hesse, 1999]. We also use in the Table below the values, based on the Figures. 3: $2J_1=2\cdot2.8\cdot10^2$ kA for the PSR phase and $2J_2=2\cdot9.11\cdot10^2$ for the TLR phase. The factor 2.0 supposes that, during the equinox, two hemispheres create equal contributions to the SCW FAC [Papitashvili et al., 2002].

4. Discussion

[10] The calculation results, and, first of all, the values of the disrupted magnetic field and the powers of the SCW disrupting processes, were used to compare the obtained PSR and TLR parameters. To estimate the reliability of the estimates, listed in the Table by using the J_y data, a portion of the results was compared to the available observational data from the literature.

Two values of the disrupted magnetic field B_{zy}, calculated for PSR and TLR on the basis of the equations (4) – (9) (Table, line 5), are compared to the corresponding data of B_m from the empirical models of the lobe magnetic field. We found that the difference of the disrupted (B_{zy}) and undisrupted magnetic fields (B_m) do not exceed 10% for TLR, but the disrupted field five

times less than undisrupted one for PSR (Table, line 8).

[11] The induction Emf in the disruption region and ΔU values (lines 9, 10) are close to the similar results Lu et al. [2000]. The disturbance global power is calculated as the sum of losses in the ionosphere, cross-tail current, and ring current, $Q=Q_i+2Q_{DR}$ (it is roughly supposed $Q_{DR}=Q_T$, [see, e.g., Turner et al., 2001; Ostgaard et al., 2002]). The obtained global Q values are agreed with the calculated values, $3Q_{SCW,}$ of the threefold power consumed in SCW (Table, lines 11, 12), where the factor 3 in front of the Q_{SCW} is, roughly, the ratio of the areas of the I-P R1 FAC, to the SCW area.

[12] Further, the data from Figure 1, according to which the observed (not calculated on the basis of the above given equations!) ΔΨ decrease for the TLR, (1835-1855) UT, is $\Delta\Psi=1.1\cdot10^8$ Wb. With due regard for $\Delta S=8.1\cdot10^{15}$ m^2, we obtain the disrupted magnetic field on the area ΔS, equal to $Bz_2=\Delta\Psi/\Delta S=(B_{zx}^2+B_{zy}^2)^{1/2}=$ 13.0 nT (Table, line 6). This estimate of B_{z2} agrees within factor <2 with the values of the undisrupted field B_m in the tail, according to the empirical models where B_m=25.0 nT [Slavin et al., 1985; Nakai a. Kamide, 1999; Shukhtina et al., 2006] (Table, line 7).

It is interesting that for the 27/08/01 event we had B_{z2}=25 nT=B_m [Mishin et al., 2008] but for the 14/09/04 event we have B_{z2}=13 nT~0.5B_m. It means that the MIT value of ΔΨ decrease for the TLR was, roughly, in two times smaller for 14/09/04 substorm than for the 14/09/04 event, although activity levels

(AE indices) were roughly the same. This discrepancy can be explained by using equation for the Poynting flux into the geomagnetosphere, $\varepsilon^*=\Psi\cdot V\langle B_L\rangle/2\mu_0$, B_L is the mean (over the tail's volume) value of the tail lobe magnetic field [e.g., Kuzminykh et al., 2008]. During the 14/09/04 event, a strong twisting of the tail magnetic field was observed (see Figure 4), in contrast to the 27/08/01 event. It might give a greater values of B_L for 14/09/04 substorm, but a smaller values of Ψ and ΔΨ.

[13] One can see that the results obtained on the basis of J_y, are in agreement with their independent analogs from the literature, that is, the differences between the two analogs are compatible with probable errors of each of them. On the other hand, the above mentioned values of the PSR and TLR main parameters, including the values of the disrupted magnetic field and the power of disruption in SCW, differ (PSR versus TLR) in many times or by order of magnitude in the case under consideration.

5. Conclusions

[14] The similar conclusions were obtained on the basis of J_x in present study and from data of 27 Aug 2001 events, during which, also, the PSR and TLR were observed as two components of one substorm [Mishial, 2008]. Thus, the described differences between the two ratios $Q_{SCW}/3Q$ for the PSR and TLR, and between two ratios B_{zy}/B_m for the PSR and TLR were observed in both events, which were considered by us.

In general, the results of this paper support the synthesis of the substorm alternative models mentioned in the Introduction. For the first time, as far as the authors are aware, we obtained the estimates of the PSR and TLR parameters, including those of the disrupted magnetic field and the power of the SCW. These estimates differ for PSR and TLR in several times or by order of magnitude.

[15] The results referring to J_x are not included in the present paper because of the limited space of the paper. They will be presented in the next paper by Mishin et al.

Table. The Parameters of the Y- Cross-Tail Current Disruption Region,

$J_Y=2J_+\cdot\sin\alpha$	PSR (α=40°) (1730-1825)UT	TLR (α=45°) (1825-1930)UT
1. SCW downward FAC intensity, $\langle 2J_+\rangle$, (disrupting FAC)	560kA	1822kA
2. Open magnetic flux ΔΨ in the tail lobe (by MIT date)		$\Delta\Psi=1.1\cdot10^8$Wb
3. The X-size of the SCW disruption region	X=-5 to -15Re	X=-5 to -35 Re
4. The Y-size of the SCW disruption region	Y=-5 to 5 Re	Y=-5 to 5 Re
5. Disrupted magnetic field, $B_{zy}=2\mu_0J_+\sin\alpha/Y$	$Bz_{1,Y}$ =7.1 nT	$Bz_{2,Y}$=25.4 nT
6. Disrupted magnetic field, $Bz_2=\Delta\Psi/\Delta S$		13nT
7. Undisrupted magnetic field (*from EM*)*	44nT	25nT
8. Ratio of the disrupted magnetic field to undisrupted one	0.16	1.01
9. Disrupted magnetic flux $F_Y=2\mu_0 J_+\sin\alpha\cdot X$	$F_{1,Y}=2.8\cdot10^7$ Wb	$F_{2,Y}=3.1\cdot10^8$ Wb.(on S_2)
10. Inductive Emf $\Delta U_Y=F/\Delta t$	$\Delta U_{1,Y}=4.6\cdot10^4$ Volt	$\Delta U_{2,Y}=2.6\cdot10^5$ Volt (on S_2)
11. Power $Q_Y=(4\mu_0J_+^2\sin\alpha\cdot X)/\Delta t$	$Q_{1,Y}=2.6\cdot10^{10}$ Watt	$Q_{2,Y}=4.7\cdot10^{11}$ Watt (on S_2)
12. Global power $Q_{T,Y}=2Q_{DR}+Q_i$	$1.2\cdot10^{12}$W	$1.8\cdot10^{12}$W
13. Disrupting current thickness $Z=2Q_{SCW}\mu_0/(S\langle Bz\rangle^2)$	$3.3\cdot10^3$ km	$1.5\cdot10^3$ km
14. Ratio of the power in the disruption region in SCW to the global power with the coefficient 0.25	0.13	1.3

EM*) – the empirical model of the undisrupted tail magnetic field from [Slavin et al., 1985; Nakai a. Kamide, 1999; Shukhtina et al., 2005].

Acknowledgement This work was supported by the grant RFBR 05-05-65170-a, INTAS 06-100013-8823, RFBR-Mong_a 08-05-90207. The authors are grateful to the colleagues of the ISTP MIT group A.D. Bazarzhapov, T.I Saifudinova Yu.A. Karavaev for a technical help. The authors thank: for providing the ACE and Wind data Drs D.McComas, R.Lepping, K.Ogilvie, J. Stenberg and A.Lasarus; for providing the

geomagnetic data Drs A.Viljanen (Image team), J. Posch (MACCS team), T.Iyemori (WDC-C2), K.Yumoto (Nagoya Univ.), O.Troshichev (AARI), E. Donovan and F. Crentzberg (CANOPUS), E.Kharin (WDC-B), B.M.Shevtsov and A.Vinnitskiy (IKIR); and PIs of the projects INTERMAGNET, GIMA (Alaska Univ.), DMI (Copenhagen), IKFIA (Yakutsk); S.Khomutov (obs. Novosibirsk), O.Kusonskiy (obs. Arti).

References

Akasofu, Source of auroral electrons and magnetospheric substorm (2003), *J. Geophys Res., 108, A4, doi: 10.1029/2002A009547.*

Baker, D.N., Pulkkinen, T.I., Angelopoulos, V., et al. (1996), Neutral line model of substorms: Past results and present view, *J. Geophys. Res., 101, 12975.*

Baker D.N., W.K. Peterson, S. Eriksson, et al. (2002), Timing of magnetic reconnection initiation during a global magnetospheric substorm onset, *Geophys. Res. Lett., 29(24), 2190, doi:10.1029/2002GL015539.*

Birn J., M. Hesse, G.Herendel, W. Baumjohann,and K. Shiokawa (1999), Flow braking and the substorm current wedge, *J. Geophys. Res., 104, A9, 19895.*

Cao, X., Z.-Y. Pu, V. M. Mishin, et al. (2008), Two case studies, *J. Geophys. Res., doi:10.1029/2007JA012761.*

Cheng C.C., C.T. Russell, M.Connors, P.J. Chi (2002), Relationship between multiple substorm onsets and the IMF: A case study, *J. Geophys. Res., 107, No A10, 1289, doi:10.1029/2001JA007553.*

Coumans V., C. Blockx, J.-C. Gerard, B. Hubert, and M. Connors (2007), Global morphology of substorm growth phases observed by the IMAGES-112 imager, *J. Geophys. Res.,112, A11211, doi: 10.10209/2007AO12329.*

Koskinen, H.E.J., R.E. Lopez, et al. (1993), Pseudobreakup and Substorm Growth Phase in the Ionosphere and Magnetosphere, *J. Geophys. Res., 98, A4, 5801.*

Lee Y., L. R. Lyons, J. M. Weygand, and C.-P. Wang (2007), Reasons why some solar wind changes do not trigger substorms, *J. Geophys. Res., doi: 10.10209/2007AO12249.*

Liang J. and W.W. Liu (2007), A MHD mechanism for generation of the meridional current cystem during substorm expansion phase, *J. Gephys. Res,, 112, A09208, doi: 10.1029/2007JAO12303.*

Lu Gang, M. Brittnacher, G. Parks, and D. Lummertzheim (2000), On the magnetospheric source egions of substorm related field-aligned currents and auroral precipitations, *J. Geophys. Res., 105, A8, 18,483.*

Lui, A.T.Y. (2001), Current controversies in magnetospheric physics, *Rev. Geophys. 39, 535-563.*

Lui A. T. Y., Y. Kamide (2003), A fresh perspective of the substorm current system and its dynamo, *Geophys. Res. Letters, 30, NO. 18, doi: 10.1029/2003GLO017835.*

Mishin, V.M. (1990), The magnetogram inversion technique and some applications, *Space Sci. Rev. 53, 83-163.*

Mishin, V.M., S.B. Lunyushkin, D. Sh. Shirapov, and W. Baumjohann (1986), A new Method for generating instantaneous ionospheric conductivity models using ground-based magnetic data, *Planet. Space Sc., 34, No. 8, 713-732.*

Mishin V M. ,L.P. Block, A.D. Bazarhapov, T.I. Saifudinova, S.B. Lunyushkin, D.Sh. Shirapov, J. Woch, L. Eliasson, G. T. Marklund, L.G. Blomberg, and H .Opgenoorth,(1997), A Study of the CDAW9C Substorm, May 3, 1986 using magnetogram inversion technique 2, and a substorm scenario with two active phases. J. Geophys. Res., **102**: 19845.

Mishin V.M., Saifudinova T.I., Bazarzhapov A.D., Russell C.T., Baumjohann W., Nakamura R., Kubyshkina M. (2001), Two distinct substorm onsets. J. Geophys/ Res., V.106, No 7, p.13105-13118.

Mishin V., Z. Pu, L. Sapronova, Y. Ku'zminykh, X. Cao and H. Zhang (2008), Active phase of a substorm is the chain of two independent types of a reconnection – in the closed plasma sheet, and open lobes of the tail, *J. Geophys. Res., (submitted)*

Miyashita Y., Y. Kamide, S.Machida, et al. (2004), Difference in magnetotail variations between intense and weak substorms, *J. Geophys. Res., 109, A11205, doi:10.1029/2004JA010588.*

Nagai T., M., Y.Saito, Fujimoto S., et al. (1998), Structure and dynamics of magnetic reconnection for substom onset with GEOTAIL observations, *J. Geophys. Res., 103, 419.*

Nakamura R., D.N. Baker, R.D. Belian, et al. (1994), Particle and field signatures during pseudo-breakup and major expansion onset, *J. Geophys. Res., 99, A1 , 207.*

Nakamura R., W. Baumjohann, Y. Asano, A. Runov, et al. (2006), Dynamics of thin current sheet associated with magnetotail reconnection, *Journal of Geophysical Research, 111, A11206, doi: 10.1029/2006JAO11706.*

Nakai H. and Y.Kamide (1999), Dependence of the near-Earth magnetotail field on storm and substorm activity, *J. Geophys. Res., 104, A10, 22,701*

Nakai H. and Y.Kamide (2004), A critical condition in magnetotail pressure for leading to a substorm expansion onset: Geotail observations, *J. Geophys. Res., 109, A0205, doi:10.29/2003JA010070.*

Ostgaard, N., Germany, G., Stadnes, J. et al. (2002), Energy analysis of substorms based on remote sensing techniques, solar wind measurements, and geomagnetic indices**,** *J. Geophys. Res. 107(A9), 1233, doi:10.1029/2001JA002002.*

Papitashvili, V.O., F. Christensen, and T. Neubert (2002), A new model of field-aligned current, *Geophys. Res. Lett., 29, 10.29/2001GLO4207.*

Papitashili V. and D.Weimer (2003), New terminology for the high-latitude field-aligned current systems, *AGU Fall Meeting, San Francisco.*

Rostoker G. (1998), On the place of the pseudo-breakup in the magnetospheric substorm, *Geophys Res. Lett., 25, NO. 2, 217-220.*

Slavin J.A., P.W. Dayly, E.J. Smith, et al. (1987), Magnetic configuration of the distant plasma sheet: ISEE 3 observations, in *Magnetotail Physic, edited by A.T.Y. Lui, p.96.*

Shukhtina M.A., N.P. Dmitrieva, and V.A. Sergeev (2004), Quantitative magnetotail characteristics of different magnetospheric states, *Annales Geophysicae, 22, 1019-1032.*

Shukhtina M.A, N.P.Dmitrieva, N.G.Popova, V.A.Sergeev, A.G. Yahnin, and I.V.Despirak (2005), Observational evi dence of the loading –unloading substorm scheme, *Geophys Res. Lett., 32, L17107, doi:10.1029/2005GL023779.*

Turner N.E., D.N. Baker, T.I. Pulkkinen, J.L.Roeder, J.F. Fennell, and V.K. Jordanova (2001), Energy content in the stormtime ring current, *J. Geophys. Res., 106, 19, 149.*